

Preparation and characterization of $[(LL)Cl_2Mo]_2(\mu-SPr)_2$ compounds with $Pr = n\text{-propyl}$ and $LL = PrSCH_2CH_2SPr$ and $Et_2PCH_2CH_2PEt_2$. Further examples of C–S bond cleavage and oxidative addition across an Mo–Mo quadruple bond

Joseph L. Deavenport, R. Theron Stubbs and Gregory L. Powell*

Department of Chemistry, Abilene Christian University, Abilene, TX 79699 (USA)

Eric L. Sappenfield and Donard F. Mullica*

Department of Chemistry, Baylor University, Waco, TX 76798 (USA)

(Received June 18, 1993, revised September 23, 1993)

Abstract

Two dimolybdenum(III) complexes with edge-sharing bioctahedral geometries have been synthesized and structurally characterized by three-dimensional, single-crystal X-ray diffractometry. Both $[(PrSCH_2CH_2SPr)Cl_2Mo]_2(\mu-SPr)_2 \cdot 0.5CH_2Cl_2$ and $[(Et_2PCH_2CH_2PEt_2)Cl_2Mo]_2(\mu-SPr)_2$ where Pr is $n\text{-propyl}$ and Et is ethyl (hereafter referred to as **1** and **2**, respectively) crystallize in the monoclinic system with two formula units per cell ($C2/m$ and $P2_1/c$, respectively). The Mo–Mo bond distances of 2.682(6) Å for **1** and 2.769(1) Å for **2** are characteristic of Mo–Mo double bonds. Bond lengths and angles are internally consistent and the van der Waals interactions are normal. Utilizing cone angle calculations, a ‘ligand profile’ describes the steric bulk about the phosphorus atoms in **2** looking down the Mo–P bonds. The resulting maximum half cone angles, $\theta/2$, are $62 \pm 1.0^\circ$. Compound **1** was prepared by a reaction involving carbon–sulfur bond cleavage, and separately, by a reaction involving oxidative addition of $PrSSPr$ across the Mo–Mo quadruple bond in $Mo_2Cl_4(PrSCH_2CH_2SPr)_2$. Compound **2** was prepared from compound **1** by ligand substitution.

Key words: Crystal structures; Molybdenum complexes, Sulfide complexes, Dinuclear complexes

Introduction

Transition-metal complexes with edge-sharing bioctahedral structures have been the subject of a number of recent studies [1–10]. Of particular interest is the extent to which metal–metal bonding occurs in these binuclear compounds, since M–M bond orders ranging from 0 to 3 are possible [11]. In the case of dimolybdenum(III) complexes, significant metal–metal bonding is usually observed with Mo–Mo distances falling in the range 2.47–2.80 Å [1, 2, 4]. However, at least one such complex is known to have an Mo–Mo distance of 3.730(1) Å and no metal–metal bond [3]. It has been suggested that subtle changes in the electronic and steric properties of the ligands are responsible for loss of metal–metal interaction. Herein, we report the synthesis and structural characterization of two new dimolybdenum(III) complexes with edge-sharing bioctahedral structures and compare their structural features with those previously reported.

Several years ago, edge-sharing bioctahedral complexes of the type $[(LL)Cl_2Mo]_2(\mu-SR)_2$, where $R = Et$ or Ph , were prepared by the oxidative addition of organic disulfides (RSSR) across the quadruple bond in $(LL)Cl_2Mo \leftarrow MoCl_2(LL)$ complexes, where $LL = 3,6\text{-dithiaoctane (dto)}$, $4,7\text{-dithiadecane (dtd)}$ and $1,2\text{-bis(dimethylphosphino)ethane (dmpe)}$ [12]. Two of these complexes (one with $R = Et$, $LL = dto$ and the other with $R = Et$, $LL = dmpe$) were characterized by X-ray crystallography and both were shown to possess a central, planar $(LL)MoS_2Mo(LL)$ unit with two chlorine atoms above and two below this plane. In contrast, an analogous dirhenium(III) compound, $[(dto)Cl_2Re]_2(\mu-SEt)_2$, was recently found to display a different ligand arrangement in which two of the chlorine atoms lie within a planar $ClSR_eS_2ReSCl$ unit, while the other two chlorine atoms lie above this plane [13]. The dimolybdenum(III) complex $[(dto)Cl_2Mo]_2(\mu-SEt)_2$

tahedral structures and compare their structural features with those previously reported.

*Authors to whom correspondence should be addressed.

was originally synthesized by a carbon–sulfur bond cleavage reaction between dtd and $[\text{Cl}_4\text{Mo}^{\pm}\text{MoCl}_4]^{4-}$, while the dirhenium(III) complex $[(\text{dto})\text{Cl}_2\text{Re}]_2(\mu\text{-SEt})_2$ could only be prepared by reaction of $[\text{Cl}_4\text{Re}^{\pm}\text{ReCl}_4]^{2-}$ with EtSSEt in the presence of dtd. In this paper, we describe two new $(\text{LL})\text{Cl}_2\text{Mo}(\mu\text{-SR})_2\text{MoCl}_2(\text{LL})$ compounds for which $\text{R}=\text{Pr}$ and $\text{LL}=\text{dtd}$ or 1,2-bis(diethylphosphino)ethane (depe), one of which was prepared by an oxidative addition reaction as well as by a reaction involving carbon–sulfur bond cleavage. To our knowledge, no dimolybdenum(III) complexes containing dtd, depe or SPr ligands have heretofore been structurally characterized.

Experimental

1,2-Bis(diethylphosphino)ethane (depe) was purchased from Strem Chemicals, Inc., and 4,7-dithiadecane (dtd) from Columbia Organic Chemical Co., Inc. All preparations were carried out in HPLC grade solvents from Aldrich Chemical Co. The dimolybdenum compounds $(\text{NH}_4)_5\text{Mo}_2\text{Cl}_9\cdot\text{H}_2\text{O}$ [14] and $\text{Mo}_2\text{Cl}_4(\text{dtd})_2$ [15] were prepared according to published procedures. All preparations were carried out under dry, positive pressure nitrogen. Visible spectra were recorded on a Perkin-Elmer Lambda 5 spectrophotometer.

Preparation of $\text{Mo}_2(\mu\text{-SPr})_2\text{Cl}_4(\text{dtd})_2$ (1)

Reaction of $[\text{Mo}_2\text{Cl}_8]^{4-}$ with dtd

A mixture of $(\text{NH}_4)_5\text{Mo}_2\text{Cl}_9\cdot\text{H}_2\text{O}$ (0.6192 g, 1.000 mmol), dtd (1.91 ml, 10.0 mmol), and methanol (30 ml) was refluxed for 22 h in an oil bath at 80 °C. The reaction was allowed to cool slowly to room temperature. After cooling, the mixture was filtered in air through a medium glass frit. A fine yellow–brown precipitate of **1** was obtained. The product was rinsed with 20 ml ethanol, and dried in a vacuum desiccator. Yield 0.25 g (30%). *Anal.* Calc. for: C, 31.43; H, 5.99; S, 22.88%. Found: C, 31.68; H, 6.04, S, 22.65%.

Reaction of $[\text{Mo}_2\text{Cl}_8]^{4-}$ with PrSSPr and dtd

A mixture of $(\text{NH}_4)_5\text{Mo}_2\text{Cl}_9\cdot\text{H}_2\text{O}$ (2.4770 g, 4.001 mmol), dtd (2.00 ml, 10.4 mmol), propyldisulfide (PrSSPr) (1.88 ml, 12.0 mmol), 5 drops concentrated HCl and methanol (45 ml) was refluxed for 2 h in an oil bath at 78 °C. The mixture was allowed to cool slowly to room temperature overnight, then filtered through a medium glass frit. The resulting solid was rinsed with 20 ml ethanol, dried in a vacuum desiccator, and characterized by Vis spectroscopy. Yield 2.52 g (75%).

Reaction of $\text{Mo}_2\text{Cl}_4(\text{dtd})_2$ with PrSSPr

A mixture of (0.2763 g, 0.40 mmol) $\text{Mo}_2\text{Cl}_4(\text{dtd})_2$, propyldisulfide (0.14 ml, 0.89 mmol) and dichloromethane (20 ml) was refluxed for 2 h. The reaction mixture was cooled to room temperature, and 20 ml of hexane was added. The mixture was filtered through a medium glass frit, an additional 20 ml of hexane was added to the filtrate, and this solution was filtered again. A yellow–brown precipitate of **1** was obtained, rinsed with ethanol, dried in a vacuum desiccator, and characterized by Vis spectroscopy. Yield 0.22 g (55%). The crystals used for the X-ray crystallographic analysis were obtained from a solution of compound **1** in dichloromethane that was allowed to slowly evaporate in open air.

Preparation of $\text{Mo}_2(\mu\text{-SPr})_2\text{Cl}_4(\text{depe})_2$ (2)

A mixture of $\text{Mo}_2(\mu\text{-SPr})_2\text{Cl}_4(\text{dtd})_2$ (0.1292 g, 0.15 mmol), 1,2-bis(diethylphosphino)ethane (0.61 mmol) and dichloromethane (20 ml) was refluxed for 21 h. There was no formation of precipitate, therefore the solution was concentrated to 50% of the original volume. To the concentrated solution, 20 ml of hexane was added to precipitate the product. The resulting solid was collected on a medium glass frit, and dried in a vacuum desiccator. Yield 0.12 g (87%). *Anal.* Calc. for: C, 34.83; H, 6.97; S, 7.15%. Found: C, 34.88; H, 6.99; S, 7.00%. The crystals used for the X-ray crystallographic analysis were obtained from a dichloromethane solution of compound **2** that was layered with hexane.

Crystallographic analysis

Conoscopic studies of single crystals of the title compounds provided evidence that the systems were biaxial (anisotropic in nature, optically birefringent). The flotation method was employed to determine the experimental densities for **1** and **2**, 1.34(2) and 1.48(2) Mg m^{-3} (calc. 1.360 and 1.509 Mg m^{-3}), respectively. Single crystals of **1** and **2** chosen on the basis of optical homogeneity were mounted on an Enraf Nonius CAD4-F autodiffractometer (Mo $\text{K}\alpha$, $\lambda=0.71073$ Å, 292 K). Three irregular-shaped crystals of compound **1** were used for the data collection due to X-ray beam sensitivity. The three data sets were corrected for decay (maximum correction of 1.46908, a mean loss in intensity of 27.2%) and Lorentz and polarization effects and then merged based on the intensity ratios of 50 reflections [16]. An empirical absorption correction was not feasible because of the decay process. Compound **2** was quite stable and therefore the data afforded a better structural solution ($R=0.050$) than that of **1** ($R=0.115$). Accordingly, only discussions related to the experimental procedures and results of **2** are presented. Nevertheless, Table 1 lists experimental and statistical summaries for

TABLE 1. Experimental and statistical summaries of **1** and **2**

	1	2
Formula	C ₂₂ H ₅₀ Cl ₄ Mo ₂ S ₆ · 0.5CH ₂ Cl ₂	C ₂₆ H ₆₂ Cl ₄ Mo ₂ P ₄ S ₂
Crystal system	monoclinic	monoclinic
Space group	C2/m (No. 12, C _{2h} ³)	P2 ₁ /c (No. 14, C _{2h} ⁵)
Radiation	Mo K α	Mo K α
$\lambda_{\text{me.an}}$ (Å)	0.71073	0.71073
T (K)	292	292
a (Å)	10.76(2)	10.705(4)
b (Å)	16.72(3)	20.285(2)
c (Å)	12.14(8)	10.213(2)
β (°)	99.3(3)	117.25(2)
V (Å ³)	2156(4)	1971.6(9)
D_m (Mg m ⁻³)	1.34(2)	1.48(2)
D_x (Mg m ⁻³)	1.360	1.509
M_r	883.2	896.4
Z	2	2
$F(000)$ (e ⁻)	902	924
μ (Mo K α) (mm ⁻¹)	1.17	1.17
$\Delta\theta$ (°)	1.5–20.0	1.5–25.0
$\Delta\omega$ (°) (ω -2 θ)	1.35° + 0.34 tan θ	1.30° + 0.34 tan θ
R_{int}	0.038	0.039
R	0.115	0.050
R_w (R_{all})	0.118 (0.176)	0.059 (0.076)
g (e ⁻²) ($\times 10^{-4}$)	3(2)	2(1)
Residual density (e ⁻ Å ⁻³)		
max.	2.33	1.14
min.	-0.80	-0.69
GOF (Σ_2)	2.50	1.24

TABLE 2. Fractional atomic coordinates ($\times 10^3$) and equivalent isotropic displacement coefficients ($\times 10^2$) for compound **1**

	x	y	z	U_{eq}^a (Å ²)
Mo	0	80(1)	0	6(1)
S(1)	79(1)	0	-135(1)	6(1)
S(2)	90(1)	196(1)	-102(1)	8(1)
Cl(1)	198(1)	101(1)	120(1)	8(1)
C(11)	260(4)	0	-97(6)	13(11)
C(12)	310(6)	0	-187(6)	21(4)
C(13)	450(4)	0	-178(6)	12(3)
C(21)	-2(4)	218(3)	-234(3)	12(2)
C(22)	48(6)	265(3)	-312(3)	16(3)
C(23)	136(7)	230(4)	-362(6)	16(3)
C(3)	62(3)	281(2)	-19(4)	14(2)
C(9) ^b	187(7)	0	446(22)	18(6)
Cl(9) ^b	305(6)	63(3)	464(3)	19(3)

^a U_{eq} is the isotropic equivalent thermal parameter and is defined as one-third of the trace of the orthogonalized U_{ij} tensor.

^bSolvent molecule solved with site occupancy = 1/4.

both studied systems and Table 2 presents the fractional atomic coordinates for compound **1**. The intensity data were collected over the range $3.0 < 2\theta < 50.0^\circ$ employing the ω -2 θ scan technique at a varied scan rate (0.49 to $3.44^\circ \text{ min}^{-1}$ in ω) which was determined by a fast prescan of $3.44^\circ \text{ min}^{-1}$. The scan range (ω) was $1.30^\circ + 0.34 \tan\theta$. All reflections having less than 75

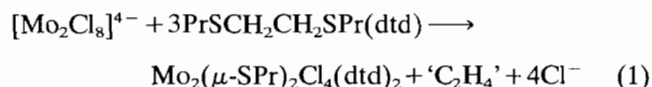
counts above background during the prescan were deemed unobserved. Periodic intensity measurements of two control reflections, monitored at 2 h intervals of collection time, revealed no sign of deterioration. Thus, the electronic hardware reliability and crystal stability were confirmed. Of the 3058 collected reflections, 2818 were independent. After averaging ($R_{\text{int}} = 0.039$), 2232 reflections fitted $F > 6.0\sigma(F)$ and were included in the structural analysis. The standard deviations of the averaged data were determined as $\sigma(F_i) = \Sigma[1.02(F_i)]/N$, where N is the number of independent measurements and $\sigma(F_i)$ is the standard deviation for each individual measurement. Lorentz and polarization corrections were applied to the collected data as well as an empirical absorption correction (transmission coefficients: max. 1.386; min. 0.667) according to the program DIFABS [17]. Examination of the resultant data revealed the extinction conditions $0k0$ where $k = 2n + 1$ and $h0l$ where $l = 2n + 1$ which are consistent with space group $P2_1/c$. Additional examination using an $N(Z)$ analysis (cumulative probability distribution test) provided further evidence of a centrosymmetric system [18].

A crystallographic analysis (direct methods) of the reduced and averaged data using Siemens SHELXTL-PC [19] and electron density calculations revealed the locations of all non-hydrogen atoms. The hydrogen

atoms were generated with idealized geometry and were constrained (at 0.96 Å from the carbon atoms) to ride on their respective bonding atoms with isotropic temperature factors fixed arbitrarily at $U_{\text{iso}} = 0.08 \text{ \AA}^2$. Several cycles varying the anisotropic thermal parameters of the non-hydrogen atoms and applying secondary extinction correction (g) to the data yielded final reliability factors and a 'goodness-of-fit' value (GOF, Σ_2) of 1.24, see Table 1. The residual index factors are defined as $R = \Sigma \Delta F / \Sigma F_o$ and $R_w = \Sigma \sqrt{w} \Delta F / \Sigma \sqrt{w} F_o$, where ΔF equals $\|F_o\| - |F_c|$ and the weighting factor w is specified as $w = 1 / [\sigma^2(F_o) + 0.0037F^2]$ where $\Sigma w \|F_o\| - |F_c|$ was minimized. The number of refined parameters was 173 which generated a data-to-parameter ratio of 13:1. A final electron density map revealed a maximum peak of $1.14 \text{ e}^- \text{ \AA}^{-3}$ in the area of the molybdenum atom which is considered quite normal for heavy metal atoms. Elsewhere, only a random fluctuating background was observed. Atomic scattering factors and anomalous dispersion corrections applied to the scattering factors were taken from the usual source [20]. Final fractional atomic coordinates according to the atom labeling scheme in Fig. 1(b) and isotropic equivalent thermal parameters are listed in Table 3.

Results and discussion

The preparation of $[(\text{dtd})\text{Cl}_2\text{Mo}]_2(\mu\text{-SPr})_2$ (**1**) by three different methods mirrors the previously reported synthesis of $[(\text{dto})\text{Cl}_2\text{Mo}]_2(\mu\text{-SEt})_2$, by analogous means [12]. Especially noteworthy is the fact that carbon-sulfur bond cleavage occurs in the reaction between $[\text{Cl}_4\text{Mo}^\ominus\text{-MoCl}_4]^{4-}$ and dtd, with the net reaction given in eqn. (1).



Whereas in the case of the dto complex, the best yield for such a reaction was only 12%, complex **1** has been repeatedly obtained in 30% yield by this procedure. Although it is possible that the subtle electronic changes on going from ethyl to propyl groups allows for the carbon-sulfur bonds to be broken more easily, we believe that steric effects may be more important. Assuming that the mechanism for these reactions involves initial coordination of dithioether (SS) to give $(\text{SS})\text{Cl}_2\text{Mo}^\ominus\text{-MoCl}_2(\text{SS})$, the greater steric demands of dtd versus dto ligands could serve to activate this intermediate metal dimer toward rearrangement with formation of Mo-SR bonds. We are currently testing this idea by investigating the reactivity of $[\text{Cl}_4\text{Mo}^\ominus\text{-MoCl}_4]^{4-}$ toward a variety of dithioethers.

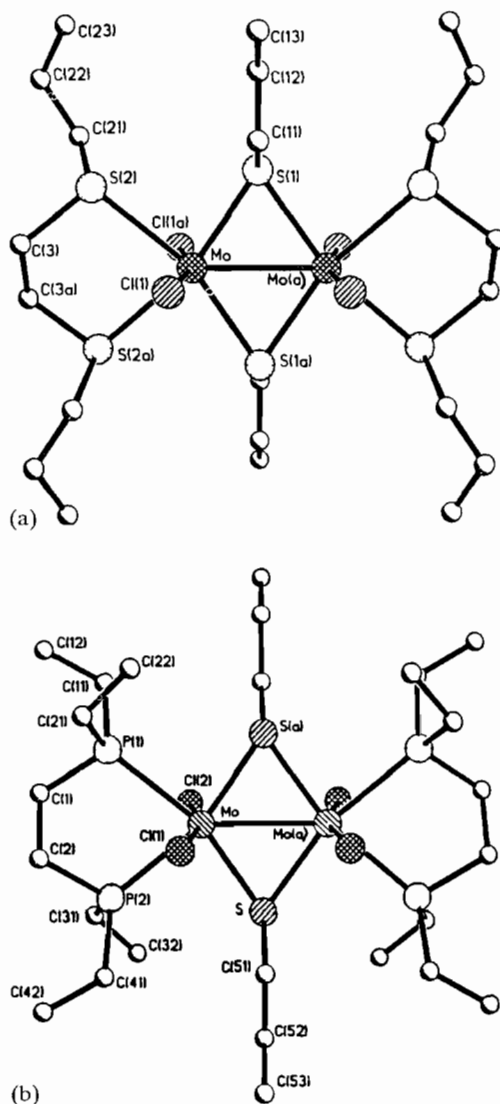


Fig. 1 Computer generated drawing of the title compounds, (a) **1** and (b) **2**, showing the atomic numbering schemes with hydrogen atoms (and solvent molecule in **1**) omitted for clarity

As mentioned, an empirical absorption correction was not possible for compound **1**, and therefore, the crystal data allowed only a crude analysis of the structure. Table 4, however, presents selective and pertinent bond distances and angles related to complex **1**, see Fig. 1(a) for labelling scheme according to Table 2. It should be stated that the component $[\text{S}_2\text{MoS}_2\text{MoS}_2]$ is planar with two chlorine atoms above and two chlorine atoms below the plane (Fig. 1(a)). Figure 2(a) is a projected view of the molecular packing.

The crystallographic data of $[(\text{depe})\text{Cl}_2\text{Mo}]_2(\mu\text{-SPr})_2$ (**2**) best fits a monoclinic lattice, space group $P2_1/c$ with two molecules per unit cell. The lack of additional symmetry elements was verified by the program MIS-SYM [21]. Figure 2(b) is a packing diagram of the contents of the unit cell. The molecules within the

TABLE 3 Fractional atomic coordinates ($\times 10^4$) and equivalent isotropic displacement coefficients ($\times 10^3$) for compound **2**

	x	y	z	U_{eq}^a (\AA^2)
Mo	5422(1)	5548(1)	907(1)	26(1)
Cl(1)	4526(2)	6403(1)	-963(2)	41(1)
Cl(2)	6560(2)	4975(1)	3227(2)	38(1)
C(1)	6010(7)	6872(4)	3476(7)	51(1)
C(2)	6823(8)	7087(4)	2678(7)	48(1)
P(1)	4565(2)	6321(1)	2346(2)	35(1)
C(11)	4070(7)	5982(3)	3700(7)	41(1)
C(12)	3887(8)	6474(4)	4719(7)	60(1)
C(21)	3174(7)	6908(4)	1321(7)	49(1)
C(22)	1794(8)	6612(4)	360(8)	70(1)
P(2)	7494(2)	6358(1)	2101(2)	34(1)
C(31)	9051(7)	6112(4)	3762(7)	55(1)
C(32)	9901(8)	5612(4)	3488(9)	67(1)
C(41)	8248(7)	6740(3)	1006(7)	41(1)
C(42)	9270(8)	7294(4)	1720(8)	64(1)
S	6825(2)	4994(1)	-47(2)	31(1)
C(51)	6921(7)	5463(3)	-1534(7)	35(1)
C(52)	8360(7)	5419(4)	-1466(7)	40(1)
C(53)	8421(7)	5825(5)	-2677(7)	57(1)

^a U_{eq} is the isotropic equivalent thermal parameter and is defined as one-third of the trace of the orthogonalized U_{ij} tensor.

TABLE 4. Interatomic bond lengths (\AA) and angles ($^\circ$) for compound **1**

Mo-Mo(a)	2.682(6)	S(1)-C(11)	1.93(5)
Mo-S(1)	2.38(1)	S(2)-C(21)	1.78(4)
Mo-S(2)	2.57(1)	S(2)-C(3)	1.79(4)
Mo-Cl(1)	2.408(8)		
S(1)-Mo-S(2)	83.5(3)	S(1a)-Mo-Mo(a)	55.7(2)
S(1)-Mo-Cl(1)	96.8(3)	S(2)-Mo-Cl(1)	79.4(3)
S(1)-Mo-Cl(1a)	92.6(3)	S(2)-Mo-Cl(1a)	88.0(3)
S(1)-Mo-S(1a)	111.3(4)	S(2)-Mo-S(2a)	82.5(5)
S(1)-Mo-S(2a)	164.1(3)	S(2)-Mo-Mo(a)	138.7(2)
S(1)-Mo-Mo(a)	55.7(2)	Mo-S(1)-Mo(a)	68.7(4)

crystal are separated by normal van der Waals contact distances, i.e., no intramolecular contact distances involving non-bonded atoms are shorter than the sum of their respective van der Waals radii. Selective bond lengths and angles are presented in Table 5. All bond distances are internally consistent and in good agreement with other experimental values found in BIDICS [22] and the Cambridge Structure Database [23]. The mean P-C bond length is 1.83(1) \AA . The phosphorus atoms are tetrahedrally coordinated with an average Mo-P-C angle (115.6 $^\circ$) larger than ideality and an average C-P-C bond angle (102.5 $^\circ$) less than ideal. These differences can be attributed to steric hindrance caused by the bulkiness of the geometry about the molybdenum atoms. The 'bite' angle of the two phosphorus atoms (P(1)-Mo-P(2), 78.3 $^\circ$) brought about by the ethane bridging which displays distinct puckering, also contributes to the angular distortions of the di-

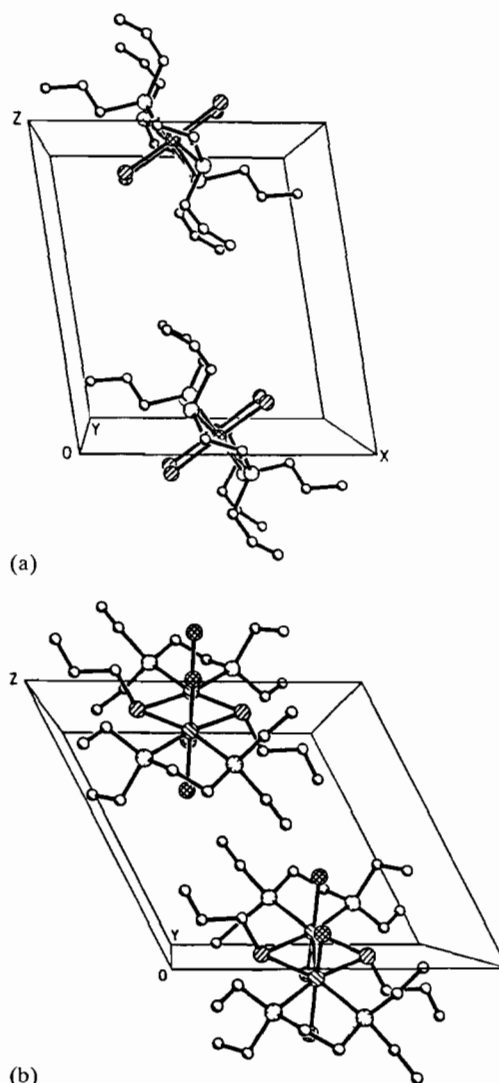


Fig. 2. The molecular packing arrangements for the asymmetric unit of (a) **1** and (b) **2** with hydrogen atoms omitted

phosphine groups. Regardless, the mean angles about atoms P(1) and P(2) are both 109.0 $^\circ$. The bond lengths associated with all hydrocarbon atoms are quite normal (mean value is 1.50 \AA). Another important structural feature is the planarity of atoms P(1), P(2), Mo, S, S(a), Mo(a), P(1a) and P(2a) with a mean deviation of 0.044 \AA and of atoms Cl(1), Cl(2), Mo, Mo(a), Cl(1a) and Cl(2a) with a mean deviation of 0.008 \AA , see Fig. 1. These planes are orthogonal, with a dihedral angle of 89.95 $^\circ$. The molecule displays an obvious and classical example of a center of inversion.

The ligand profile of the two phosphine ligands can be represented in terms of a cone angle. The steric bulk about the two phosphorus atoms is viewed down the molybdenum-phosphorus bonds. The concept of the cone angle, θ , a measure of steric bulk for phosphine ligands, was initiated by Tolman [24, 25], whose work was followed by the development of the rotational

TABLE 5 Interatomic bond lengths (Å) and angles (°) for compound 2

Mo-Cl(1)	2.427(2)	P(1)-C(1)	1.828(7)
Mo-Cl(2)	2.410(2)	P(1)-C(11)	1.826(9)
Mo-S	2.411(2)	P(1)-C(21)	1.818(7)
Mo-S(a)	2.415(2)	P(2)-C(2)	1.855(9)
Mo-P(1)	2.587(3)	P(2)-C(31)	1.821(6)
Mo-P(2)	2.574(2)	P(2)-C(41)	1.824(9)
Mo-Mo(a)	2.769(1)	C(1)-C(2)	1.504(13)
S-C(51)	1.836(8)	C(11)-C(12)	1.518(11)
C(51)-C(52)	1.512(11)	C(21)-C(22)	1.476(10)
C(52)-C(53)	1.512(12)	C(31)-C(32)	1.474(13)
		C(41)-C(42)	1.504(10)
Cl(1)-Mo-Cl(2)	163.3(1)	Mo-P(1)-C(1)	108.2(3)
Cl(1)-Mo-P(1)	84.2(1)	Mo-P(1)-C(11)	120.2(2)
Cl(1)-Mo-P(2)	82.1(1)	Mo-P(1)-C(21)	118.7(3)
Cl(1)-Mo-S	96.3(1)	C(1)-P(1)-C(11)	101.9(3)
Cl(1)-Mo-S(a)	94.0(1)	C(1)-P(1)-C(21)	101.3(3)
Cl(1)-Mo-Mo(a)	99.0(1)	C(11)-P(1)-C(21)	103.7(4)
Cl(2)-Mo-P(1)	83.4(1)	Mo-P(2)-C(2)	106.5(2)
Cl(2)-Mo-P(2)	84.5(1)	Mo-P(2)-C(31)	119.3(3)
Cl(2)-Mo-S	92.5(1)	Mo-P(2)-C(41)	120.5(2)
Cl(2)-Mo-S(a)	96.3(1)	C(2)-P(2)-C(31)	104.1(3)
Cl(2)-Mo-Mo(a)	97.7(1)	C(2)-P(2)-C(41)	101.6(4)
P(1)-Mo-P(2)	78.3(1)	C(31)-P(2)-C(41)	102.3(4)
P(1,2)-Mo-S,S(a)	164.0(1)	P(1)-C(1)-C(2)	111.6(5)
P(1,2)-Mo-S,S(a)	85.9(1)	P(1)-C(11)-C(12)	116.4(5)
P(1,2)-Mo-Mo(a)	140.8(1)	P(1)-C(21)-C(22)	115.0(6)
S-Mo-S(a)	110.0(1)	P(2)-C(2)-C(1)	110.2(5)
S-Mo-Mo(a)	55.1(1)	P(2)-C(31)-C(32)	113.1(5)
S(a)-Mo-Mo(a)	54.9(1)	P(2)-C(41)-C(42)	116.7(5)
Mo-S-Mo(a)	70.0(1)	S-C(51)-C(52)	111.9(4)
Mo-S-C(51)	111.9(2)	C(51)-C(52)-C(53)	110.7(5)
Mo(a)-S-C(51)	111.1(2)		

angle, ϕ [26–28]. A ligand profile (or silhouette profile) yields a numerical value that represents the steric bulk of the ligands. This value can then be employed to predict conformations and evaluate steric demands as well as reaction rates and mechanism. The outline (silhouette) is clearly seen in Fig. 3. The maximum (minimum) half cone angles, $\theta/2_{\max}$, about the two phosphorus atoms in this compound are both $62(37)^\circ$, e.s.d.s $\pm 1.0^\circ$. These values have been calculated from crystallographic data which also developed the polar ligand profile.

As mentioned above, two complexes of the type $[(LL)Cl_2Mo]_2(\mu-S\text{Et})_2$ with structures similar to compounds 1 and 2 were previously reported [12]. In these earlier complexes, LL is either 3,6-dithaoctane (dto) or 1,2-bis(dimethylphosphino)ethane (dmppe). All four complexes are edge-sharing bioctahedra with metal–metal double bonds, two bridging thiolates and two terminal chelating ligands. The chelates are positioned so as to occupy the furthest possible distance from each other. In each compound, the equatorial plane consists of either $[S_2MoS_2MoS_2]$ or $[P_2MoS_2MoP_2]$ and the Cl atoms lie in the perpendicular apical plane.

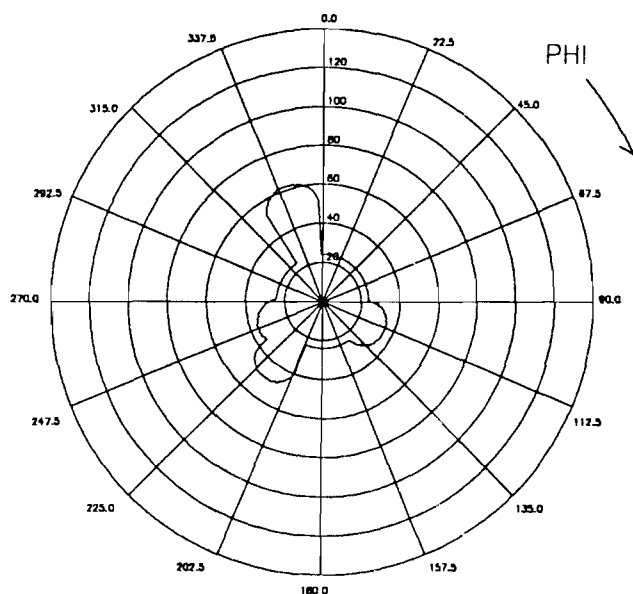


Fig. 3 Ligand profile ($\theta/2$ vs. ϕ) looking down the Mo-P(1,2) bond of compound 2. Since both profiles are precisely alike (superimposable), only one profile is shown

TABLE 6. Comparison of bond distances (Å) and angles (°) for the two dithioether complexes [(LL)Cl₂Mo]₂(μ-SR)₂, where R = Et or Pr and LL = dto or dtd

Distance or angle	[(dto)Cl ₂ Mo] ₂ (μ-SEt) ₂	[(dtd)Cl ₂ Mo] ₂ (μ-SPr) ₂ (1)
Mo–Mo	2.682(1)	2.682(6)
Mo–S _b ^a	2.402(2)	2.38(1)
Mo–S	2.579(1)	2.57(1)
Mo–Cl	2.403(1)	2.408(8)
Mo–S _b –Mo	67.90(3)	68.7(4)
S _b –Mo–S _b	112.10(3)	111.3(4)
Mo–Mo–S	138.81(3)	138.7(2)
Cl–Mo–Cl	163.04(3)	163.2(4)
Mo–Mo–Cl	98.42(3)	98.4(2)

^aS_b denotes bridging sulfur atom.

TABLE 7. Comparison of bond distances (Å) and angles (°) for the two diphosphine complexes [(LL)Cl₂Mo]₂(μ-SR)₂, where R = Et or Pr and LL = dmpe or depe

Distance or angle	[(dmpe)Cl ₂ Mo] ₂ (μ-SEt) ₂	[(depe)Cl ₂ Mo] ₂ (μ-SPr) ₂ (2)
Mo–Mo	2.712(3)	2.769(1)
Mo–S	2.411(4)	2.413(2)
Mo–P	2.541(3)	2.581(3)
Mo–Cl	2.417(3)	2.419(2)
Mo–S–Mo	68.5(1)	70.0(1)
S–Mo–S	111.5(1)	110.0(1)
Mo–Mo–P	140.3(1)	140.8(1)
P–Mo–P	79.5(2)	78.3(1)
Cl–Mo–Cl	162.9(2)	163.3(1)
Mo–Mo–Cl	98.55(8)	99.0(1)

The coordination spheres of [(dto)Cl₂Mo]₂(μ-SEt)₂ and [(dtd)Cl₂Mo]₂(μ-SPr)₂ (1) are remarkably similar. A comparison of bond distances and angles is found in Table 6. The central portions of the diphosphine complexes (Table 7) [(dmpe)Cl₂Mo]₂(μ-SEt)₂ and [(depe)Cl₂Mo]₂(μ-SPr)₂ (2) are also quite similar, but these complexes are not as closely related as the dithioether compounds. The most obvious dissimilarity is the longer Mo–Mo bond distance in compound 2 (2.769(1) Å) compared to the previously reported dmpe compound (2.712(23) Å). It seems likely that this difference is due to the greater steric bulk of the ligands in compound 2 (both of depe versus dmpe and dtd versus dto), which presumably forces the Mo atoms further apart.

The metal–metal bonding in these complexes has been described in terms of a $\sigma^2\pi^2(\delta \text{ or } \delta^*)^2$ electronic configuration, in which the weakly bonding δ and weakly antibonding δ^* orbitals are very close in energy and their ordering uncertain [12]. Thus the Mo–Mo bond order is best described as approximately 2, and the Mo–Mo distances are consistent with this assignment [1]. Also consistent with this description are the visible spectra for these complexes, which are discussed here for the first time.

Each complex exhibits a fairly strong electronic absorption maximum between 440 and 480 nm and a much weaker absorption maximum between 700 and 760 nm. For [(dto)Cl₂Mo]₂(μ-SEt)₂ and [(dtd)Cl₂Mo]₂(μ-SPr)₂ (1), the weaker absorption maximum occurs at 712 nm, while for [(dmpe)Cl₂Mo]₂(μ-SEt)₂ and [(depe)Cl₂Mo]₂(μ-SPr)₂ (2), the weak peaks are centered at 720 and 750 nm, respectively. Assuming that these absorption peaks are due to either a $\delta \rightarrow \delta^*$ or a $\delta^* \rightarrow \delta$ transition, the red shift on going from the dithioether complexes to the diphosphine complexes is easily explained. For [(dto)Cl₂Mo]₂(μ-SEt)₂ and [(dtd)Cl₂Mo]₂(μ-SPr)₂ (1), the Mo–Mo bond distances are indistinguishable at 2.68 Å, while this distance is 2.71 Å in [(dmpe)Cl₂Mo]₂(μ-SEt)₂ and 2.77 Å in [(depe)Cl₂Mo]₂(μ-SPr)₂ (2). This lengthening of the Mo–Mo bond most certainly narrows the energy gap between the δ and δ^* orbitals, since δ overlap is especially sensitive to changes in metal–metal distances. Thus the $\delta \rightarrow \delta^*$ or $\delta^* \rightarrow \delta$ transition energies for the dto and dtd complexes would be expected to be essentially identical, while this transition energy for the dmpe complex should occur at higher wavelength and that for the depe complex should fall at still higher wavelength. This is exactly what is observed.

Supplementary material

Structure factors and anisotropic thermal parameters are available from author D.F.M.

Acknowledgements

Acknowledgements are made to The Robert A. Welch Foundation (Grant Nos. AA-0668 and R-1054), Abilene Christian University and Baylor University, in part for support of this research.

References

- 1 F.A. Cotton, *Polyhedron*, **6** (1987) 667.
- 2 B.E. Owens and R. Poli, *Polyhedron*, **8** (1989) 545
- 3 H.D. Mui and R. Poli, *Inorg Chem*, **28** (1989) 3609
- 4 R. Poli and H.D. Mui, *Inorg Chem*, **30** (1991) 65.
- 5 F.A. Cotton, L.M. Daniels, K.R. Dunbar, L.R. Falvello, C.J. O'Connor and A.C. Price, *Inorg Chem*, **30** (1991) 2509
- 6 F.A. Cotton, M. Shang and W.A. Wojtczak, *Inorg Chem.*, **30** (1991) 3670
- 7 F.A. Cotton, C.A. James and R.L. Luck, *Inorg Chem*, **30** (1991) 4370.
- 8 F.A. Cotton and R.C. Torralba, *Inorg Chem.*, **30** (1991) 4392.
- 9 F.A. Cotton and S.K. Mandal, *Inorg Chem*, **31** (1992) 1267.
- 10 F.A. Cotton, J.L. Eglin and S.J. Kang, *J Am Chem Soc*, **114** (1992) 4015.
- 11 S. Shaik, R. Hoffmann, C.R. Fisel and R.H. Summerville, *J Am. Chem Soc*, **102** (1980) 4555.
- 12 (a) F.A. Cotton and G.L. Powell, *J Am Chem. Soc*, **106** (1984) 3371; (b) F.A. Cotton, M.P. Diebold, C.J. O'Connor and G.L. Powell, *J Am Chem Soc*, **107** (1985) 7438.
- 13 B.J. Heyen and G.L. Powell, *Inorg Chem*, **29** (1990) 4574.
- 14 J.V. Brenic and F.A. Cotton, *Inorg Chem*, **9** (1970) 346.
- 15 J. San Filippo, Jr., H.J. Sniadoch and R.L. Grayson, *Inorg Chem*, **13** (1974) 2121.
- 16 *Enraf-Nonius VAX Structure Determination Package*, Enraf-Nonius, Delft, Netherlands, 1983
- 17 N. Walker and D. Stuart, *Acta Crystallogr*, *Sect A*, **39** (1983) 159.
- 18 E.R. Howells, D.C. Philips and D. Rogers, *Acta Crystallogr.*, **3** (1950) 210.
- 19 *SHELXTL-PC*, Siemens Analytical X-ray Instrument, Madison, WI, USA, 1989.
- 20 J.A. Ibers and W.C. Hamilton, *International Table for X-ray Crystallography*, Vol. IV, Kynoch, Birmingham, UK, 1974, p. 72
- 21 E.J. Gabe, Y. Le Page, J.-P. Charland and F.L. Lee, *J Appl Crystallogr*, **22** (1989) 384.
- 22 *Bond Index to the Determinations of Inorganic Crystal Structures*, Institute for Material Research, Hamilton, Canada, 1968–1981
- 23 A.G. Orpen, L. Brammer, F.H. Allen, O. Kennard, D.G. Watson and R. Taylor, *J Chem Soc*, *Dalton Trans* (1989) 59.
- 24 C.A. Tolman, *J Am Chem Soc*, **92** (1970) 2956.
- 25 C.A. Tolman, W.C. Seidel and L.W. Gosser, *J Am Chem Soc*, **96** (1974) 53.
- 26 J.H. Richardson and N.C. Payne, *Can J Chem*, **55** (1973) 3203
- 27 E.C. Alyea, S.A. Dias, G. Ferguson and R.G. Restivo, *Inorg Chem*, **16** (1977) 2329
- 28 J.D. Smith and J.D. Oliver, *Inorg Chem*, **17** (1978) 2585.